INORGANIC CHEMISTRY

Lunara Rakhymbay ⬤, Bagdaulet Shugay ⬤, Maksat Karlykan, Alibi Namazbay, Aishuak Konarov* ⬤ , Zhumabay Bakenov ⬤

*Department of Chemical and Materials Engineering, School of Engineering and Digital Sciences,
Nazarbayev University, Astana, Kazakhstan
(*Corresponding author's e-mail: aishuak.konarov@nu.edu.kz)*

Recent Advances in Layered Na$_2$Mn$_3$O$_7$ Cathode Materials for Sodium-Ion Batteries

There has been an increasing amount of attention paid to the different technologies that are used in energy production and storage in the context of day-to-day operations, which range from small-scale applications to large-scale applications, which are all equally important. As far as energy storage systems are concerned, Li-ion batteries are the market leader due to their high energy and power density, making them one of the most popular choices. Despite this, a significant concern is the scarcity of lithium resources and other metals that are needed for cathode material, such as cobalt and nickel, in the long run. Recent research has focused on alternative energy storage systems to mitigate these concerns. Due to sodium's widespread availability and similar chemistry to lithium-ion batteries (LIBs), sodium-ion batteries (SIBs) are considered the most promising next-generation alternatives. Being competitive in the market today requires the development of cathode materials that are of high performance. Among the studied materials, the Na$_2$Mn$_3$O$_7$ electrode displayed high capacity. In addition, the low price of sodium and manganese makes it even more attractive. In this work, we summarized the recent progress in studying and enhancing the Na$_2$Mn$_3$O$_7$ cathode material.

Keywords: rechargeable batteries, sodium-ion battery, redox reaction, layered structure, cathode, low voltage, high voltage, oxygen redox.

Content

List of abbreviations

ESS: energy storage systems
BES: battery energy storage
SIBs: sodium-ion batteries
LIBs: lithium-ion batteries
SHE: standard hydrogen electrode

EES: electrical energy storage
HC: hard carbon
CV: cyclic voltammetry
GITT: galvanostatic intermittent titration technique
XANES: X-ray absorption near edge structure

Review Plan

Inclusion and Exclusion Criteria: The present review discussed the current progress in the sodium cathode materials, specifically the $Na_2Mn_3O_7$. The review data are based on very recent scientific publications from 2017 to 2022. Some older literature sources (2001–2013) provide information about the first attempts to synthesize $Na_2Mn_3O_7$ and other materials with oxygen redox. A large-scale study of diazonium sulfonate salts began with the work of Barbero (1998) and continues now. We searched and analyzed articles from Scopus, and Web of Science. The keywords used for the search were "sodium cathodes", "$Na_2Mn_3O_7$", "layered structure", "oxygen redox", "Manganese based", etc. The resultant data were discussed in this work. No statistical methods were used in this review.

Introduction

Modern generations use rechargeable batteries to supply power and power any modern electronics (such as mobile phones, laptops, etc.) that require electricity to function without the need for an external source of electricity [1–6]. When compared to other rechargeable battery technologies, LIBs combine the advantages of high energy density, a compact, and lightweight design, and excellent cycle life compared to other rechargeable battery technologies. However, due to the increasing number of applications, from small to a larger scale, the pressure for the production of LIBs is getting tougher every year since the resources of lithium and other transition metals such as cobalt and nickel are limited, which negatively affects the price [7–11]. This has led to an extensive study of a variety of different types of rechargeable batteries, such as the Na-, K-, Zn-, Ca-, and Mg-ion batteries, to take advantage of their availability of resources over LIBs so that they may serve as alternatives to LIBs.

In this regard, sodium-ion batteries (SIBs) possess distinct advantages over LIBs, namely relative abundance and low electrochemical potential standing at –2.71 V compared to a standard hydrogen electrode (SHE) negligibly above that of LIBs (330 mV); thus, enabling SIBs to fulfill demands for large-scale electrical energy storage (EES) [12]. The SIBs commercialized by the Faradion company can be an example of a successful trial that could surpass the energy densities of Li-ion batteries ($LiFePO_4$/graphite) with a quickly convergent cycle lifetime, comparable rate performance and charge acceptance [13]. Additionally, laminated batteries and coin cells were exemplified by Sumitomo Chemical Co. Ltd. employing O3-type $NaFe_{0.4}Mn_{0.3}Ni_{0.3}O_2$ cathode and hard carbon (HC) anode. When the laminated battery was charged beyond 200 percent of its functional capacity and reached 12 V, neither explosion nor ignition occurred. Even though these SIBs demonstrate high-rate capabilities and cycle life, they perform worse than their LIBs counterparts. Then, Faradion produced storage with an aimed capacity of 418 Wh utilizing 48 cells and a 3 Ah pouch prototype SIB to charge an electric bicycle [14]. Despite the weaknesses of SIBs lacking in LIBs, such as insufficient energy density due to low operation voltage, SIBs are still considered a prospective alternative to surpass high-cost LIBs in a large-scale application. The energy density of the battery can be enhanced by utilizing cathode materials with high redox potentials using electrode materials that possess a high specific capacity. Since most cathode materials store sodium ions through intercalation, the number of sites for storage is limited, leading to the challenge of increasing the specific capacity of cathode materials. In addition, the utilization of cathode materials with high redox potentials is restricted due to the decomposition of electrolytes at high potentials.

In this review, we have focused on $Na_2Mn_3O_7$-based cathode materials since they displayed high capacity (>200 mAh g^{-1}). Moreover, sodium and manganese are cheap elements. However, the material suffered from rapid capacity fading, which hindered its commercialization. Many approaches have been addressed, such as doping to stabilize the structure. A detailed look into these approaches will be discussed in this work.

1. A low voltage cathode: based only on Mn^{4+}/Mn^{3+} redox

The electrochemical activity of Na-Mn-O ternary layered metal oxide ($Na_2Mn_3O_7$) is an important phenomenon in the research of Mn-based cathode materials for SIBs as manganese-based cathodes have gained some attention because of its effective environmental-friendly aspect and low price. As a cathode material,

Na$_2$Mn$_3$O$_7$ possesses a layered structure where layers build by Mn-O bonds in each corner of the octahedra. As redox reaction is central chemistry, it is critical to investigate whether the intercalation and deintercalation process only with Mn^{4+} oxidation surrounded by octahedral oxygen or whether SIBs are accompanied by the release of oxygen.

As Adamczyk et al. [15] the first well-studied counterpart of sodium cathode was Li$_2$Mn$_3$O$_7$ prepared by the ionic exchange method by Raekelboom et al. [16] from Na$_2$Mn$_3$O$_7$. As synthesized material was crystallized in the layered structure with the space group of R$3m$. The assembled half-cell with Li$_2$Mn$_3$O$_7$ cathode material delivered an initial capacity of 160 mAh g^{-1}, where a plateau appears at 3.0 V. However, due to the unstable crystal structure where layered structure transferred to the spinal structure, the long-term cycling displayed poor performance. On the other hand, this phase transition is not noticed in the SIBs systems, and because of this given novelty, researchers synthesized Na$_2$Mn$_3$O$_7$ by the conventional solid-state method [15]. By sintering at 600 °C for 4 hours, they obtain the material with triclinic space group P1. Figure 1 illustrates the galvanostatic charge and discharge curves of the given material for the initial five cycles, where detected the main plateau at 2.1 V, which provides the 160 mAh g^{-1} capacity. The cyclic voltammetry peaks prove the above-detected plateau region which is consistent with the Mn^{4+}/Mn^{3+} couple. The polarization degree of described peaks was around 20 mV which was 2.1 V for the reduction peak and 2.2 V for the oxidation peak. As well known, the layers of the cathode material consist of transition metals with d orbitals. During the redox reactions, the d-orbitals mentioned above start to convert to degenerate states and, at the low voltage, lead to the asymmetrical location of transition metal layers. In the degenerate states, electrons of the d-orbital may occupy XY, XZ, or YZ orbitals. In simple words, the geometry of equatorial and axial bonds alters and leads to the shortening or elongation of axial bonds compared with equatorial bonds. Due to these changes during the cycling, the performance was not satisfying.

Recent studies by Sada et al. [17] used Na$_2$Mn$_3$O$_7$ as an appropriate positive carrier for reversible redox reactions of Li, K, and Na batteries. They cut the voltage window to 3.0 V and excluded the oxygen release. As illustrated in Figure 2, the galvanostatic experiments in the shortened voltage window started with the discharge cycle of the coin cell batteries as the oxidation state of the Mn in the cathode obtained the highest (4+) state. Figure 2 demonstrates the specific capacities where specific discharge capacities reached 160 mAh g^{-1} for Li and 140 mAh g^{-1} for Na and K batteries. Interestingly, compared to Na, and K, Li-ion exhibited a jumping of the working voltage almost to 1 V, which boosts the energy density of the lithium-based half-cell battery. However, LIBs systems exhibit irreversible phase transitions, which lead to a fast decline of the irreversible capacity in the following cycles [18].
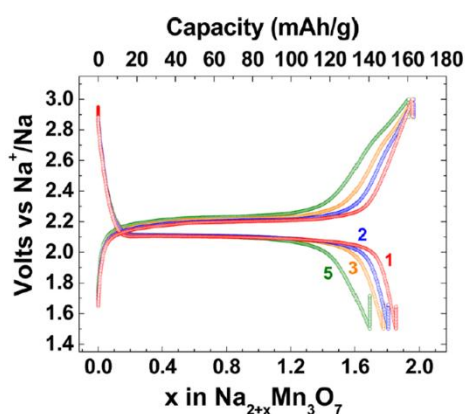

Figure 1. Galvanostatic charge and discharge profile of SIBs. Reprinted with permission from [15]. Copyright {2017} American Chemical Society
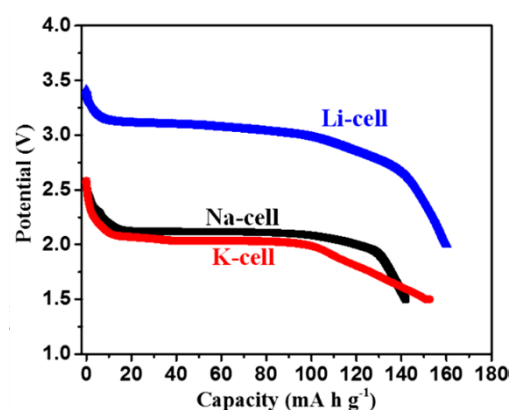
Figure 2. Comparison of the first discharge curves of Na$_2$Mn$_3$O$_7$ with Li$^+$, Na$^+$, and K$^+$ half-cells. Reprinted with permission from [19]. Copyright {2018} American Chemical Society

The studies mentioned above concerned the possibility of using Mn-based material for non-aqueous electrolyte systems where electrolytes are toxic and have safety problems because of exothermic reactions. By considering aqueous Zn-ion batteries, researchers proposed an alternative way to exclude such issues in developing Na$_2$Mn$_3$O$_7$ materials as a cathode for aqueous Zn-ion batteries [19]. In their preparation, they use

600 °C for the tablets prepared by the solid-state method. Figure 3 demonstrates the interesting phenomenon with initial discharge capacity and following increase upon cycling. This phenomenon can be explained by the low wettability degree of active material and activation of $Na_2Mn_3O_7$, followed by phase transformations illustrated in Figure 4. The characteristic peaks appeared at 1.3 and 1.44 V in the reduction reaction and symmetric peaks at 1.5 and 1.5 V in the oxidation reaction. These peaks match with the Mn^{4+}/Mn^{3+} redox reaction and provide overlapped symmetric peaks. Further cycling until 400 cycles provide a retention rate of around 65 % of the initial capacity. If we compare the energy density of non-aqueous and aqueous electrolytes for SIBs and Zn-ion batteries, we detect comparable 300-350 Wh kg^{-1} results.
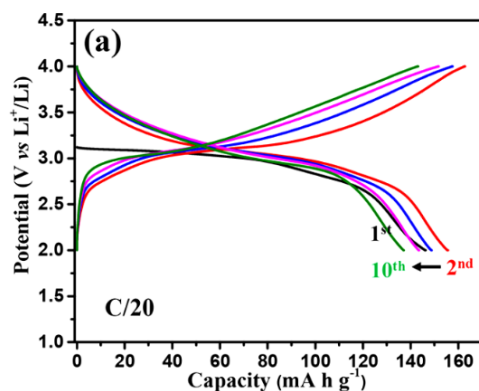

Figure 3. Galvanostatic charge and discharge curves at C/20 rate. Reprinted with permission from [19]. Copyright {2018} American Chemical Society
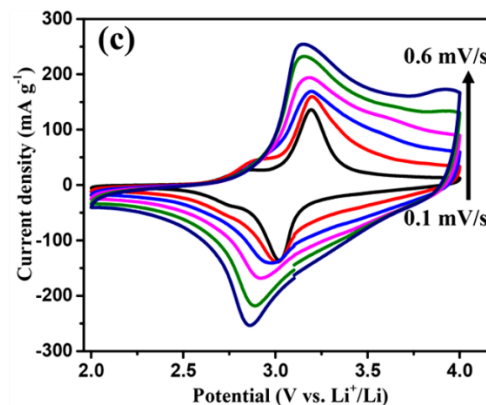
Figure 4. Cyclic voltammograms with six different scan rates from 0.1 to 0.6 mV s^{-1}. Reprinted with permission from [19]. Copyright {2018} American Chemical Society

To sum up, research on cathode for SIBs field proves the capabilities of the $Na_2Mn_3O_7$ to use as a promising candidate. The capacity of redox reaction at shortened cut-off voltage window came from reversible intercalation and deintercalation of two sodium ions through a so-called biphasic process where material structure can be explained by the formula $Na_{4.2}Mn_3O_7$ with Na^+ state. As described above, a long plateau at 2.1 V for the galvanostatic test and a peak with a low polarization in the cyclic voltammetry test provide the 160 mAh g^{-1}. With an average working voltage of 2.1 V and energy density of 330 Wh kg^{-1}, other properties such as non-toxicity, low price, and simple preparation ways increase the interest in a given material.

2. A high voltage cathode: based on the combination of Mn^{4+}/Mn^{3+} and Oxygen redox

Another interesting study indicates that when the theoretical limit of the M-redox reaction is exceeded in alkali metal excess transition metal oxides ($A_{1+x}M_{1-x}O_2$), additional capacity can be obtained as a result of additional oxygen redox reactions. [20]. A good example of this is the material $Li_{1.2}Ni_{0.13}Co_{0.13}Mn_{0.54}O_2$, where $0.2Li^+$ are located in the transition metal layer. This material delivered a specific capacity of 270 mAh·g^{-1}, of which 150 mAh·g^{-1} of capacity was derived via oxygen redox. [21]. Ceder's research group provided a theoretical explanation for reversible oxygen-redox reactions. The redox activity of oxygen in layered materials with an excess of lithium arises from Li-O-Li bonding, which creates orphan states of oxygen that rise from the oxygen-binding manifold [22]. There is still some uncertainty regarding oxygen-redox reactions, but it is generally accepted that in AMO_2, oxygen is coordinated by three transition metals, and its 2p orbitals are primarily involved in bonding states located below Fermi's level. Consequently, oxygen oxidation removes a bonding electron from an M-O bond. On the other hand, it is important to note that two transition metal atoms are coordinated by two oxygen atoms in $A_{1+x}M_{1-x}O_2$, unlike in the case of AMO_2. By having a nonbonding 2p orbital along the A-O-A axis and a position below the Fermi level, this oxygen contributes to the oxygen-redox reaction without causing M-O bonds to become easily broken [23, 24].

In 2018 Prof. Yamada's research group studied the reversible oxygen redox capacity of $Na_2Mn_3O_7$ at ≈4.1 V versus Na/Na^+, and DFT calculations were used to confirm nonbonding oxygen 2p orbitals [25, 26]. The authors predicted that oxygen has so-called nonbonding 2p orbitals in manganese vacancy, which delivers this extra capacity. As shown in Figure 5a, during the initial cycle, there were no changes in Mn L-edge, which indicates that the Mn does not contribute to the capacity. On the other hand, the O K-edge (Fig. 5b and 5c) displays that during charge, the intensity of the shoulder peak increased, and during discharge, it returned back to the initial state. These changes are associated with reversible oxygen redox. In addition to the exper-

imental data, it was confirmed by the theoretical calculations, which are shown in Figures 5d and 5e [25]. The charge-discharge curve between 1.5–3.0 V verified that reaction occurred due to $Mn^{4+/3+}$ redox, which corresponds to previous French scientist's investigations [15]. However, in this paper, they observed another part of the cut-off voltage (3.0–4.7 V) where an extra 75 mAh g^{-1} capacity (at ≈4.1 V versus Na/Na$^+$) is obtained (Fig. 6). Considering that Mn can not be oxidized upper 4+, considered that it happened due to reversible oxygen redox. Combining Mn and O redox Na₂Mn₃O₇ can deliver a high reversible capacity (>200 mAh·g^{-1}) [27].
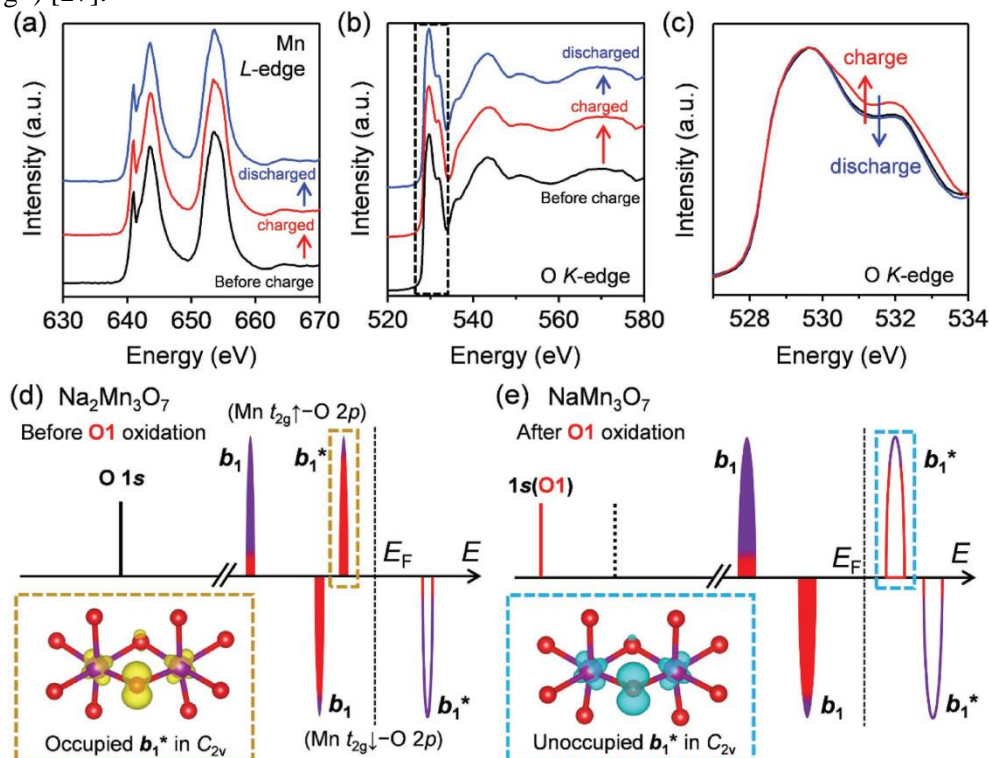

Figure 5. Electronic structure changes of Na₂Mn₃O₇ during the charge and discharge. a) Ex situ X-ray absorption spectra for Mn L3-edge. b) Ex situ X-ray absorption spectra for O K-edge. c) Enlarged part of X-ray absorption spectra for O K-edge. Schematic illustration of the electronic structures of d) Na₂Mn₃O₇ and e) NaMn₃O₇. Densities of states are labelled based on the molecular orbitals of OMn₂ in a C_{2v} symmetry. Reprinted with permission from [25]. Copyright {2018} Wiley
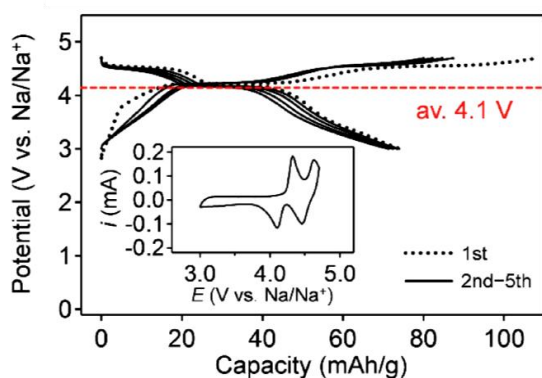

Figure 6. Galvanostatic charge/discharge curves between 3.0 and 4.7 V versus Na/Na$^+$ Reprinted with permission from [25]. Copyright {2018} Wiley
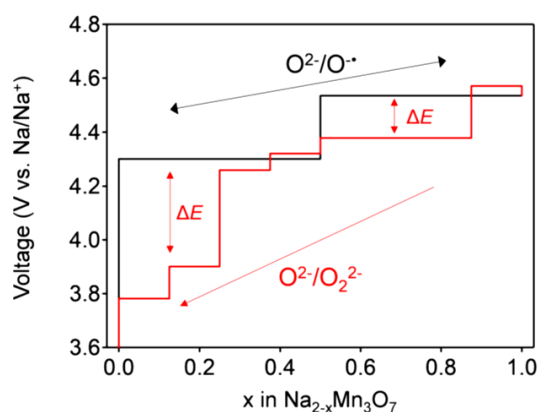
Figure 7. Predicted voltage hysteresis of Na₂₋ₓMn₃O₇ with hypothetical peroxide-like O₂$^{2-}$ dimers. Reprinted with permission from [26]. Copyright {2021} Springer Nature

Even so, the chemical state of oxidized oxygen in this material is still debatable. Because of the high voltage hysteresis (|rGox | |rGred |), oxidized oxide ions (O•) form stable peroxide-like O₂$^{2-}$ dimers when

charged. Following discharge, the O_2^{2-} dimer may be reduced to O_2^{4-} and then decomposed to O_2. In addition, this hysteresis, when transition-metal migration and/or surface cation densification happen simultaneously, the overlapping kinetic hysteresis caused by concentration overpotential, makes overall mechanisms challenging [28].

The $Na_{2-x}Mn_3O_7$ was recently investigated to exhibit a high reversible oxygen-redox capacity with little voltage hysteresis (0.04 V) and thus a good counterpart (Fig.7), |rGox | |rGred |) for gaining an understanding of the cause of the normally high voltage hysteresis observed following oxygen redox. Why $Na_{2-x}Mn_3O_7$ exhibits the reversible oxygen-redox reaction in this mechanism $O^{2-}/O^{-\bullet}$? To answer this question, Prof. Yamada's group again investigated this material and aimed to confirm the existence of $O^{-\bullet}$ in $Na_{2-x}Mn_3O_7$ as the dominant state in the reversible oxygen redox in the thermodynamical view of analysis. By the DFT calculation, it was confirmed that the calculated magnetic moments of Mn and O gradually appear on O atoms during dissociation, which indicates the formation of $O^{-\bullet}$. In comparison, the multiorbital Mn-O bond (($\sigma + \pi$) helps to stabilize the formed $O^{-\bullet}$ in the structure $Na_{2-x}Mn_3O_7$ [26].

Partially substituting the Mn^{4+} with other elements with different oxidation states, such as Mg^{2+}, Al^{3+}, Ti^{4+}, etc., is one efficient method for further deeply studying the redox-active oxygen atoms. For efficient substitution, Mn and element should have similar ionic radii [24].

P. Siriwardena et al. studied a series of Mg^{2+} doped $Na_2Mn_3O_7$. The results imply that Mg^{2+} doping can positively affect capacity enhancement and rate capability. 2 mol. % Mg^{2+} doped material exhibited the best specific capacity of 143 mAh g^{-1} after 30 cycles. However, with long-term electrochemical cycling, a somewhat negative effect on capacity retention was observed, which was associated with increasing Mn^{4+} in the system. As we know that Mn^{4+} can form Mn^{2+} in an acidic solution, which can easily dissolve in the electrolyte, which causes structural instability. In addition, GITT and CV studies for NaMnO, $NaMnMg_{0.5}O$, and $NaMnMg_2O$ materials have shown that Mg^{2+} doping can reduce the Na^+ vacancy ordering, resulting in improved diffusion. Also, a $NaMnMg_{0.5}O$/ HC anode full cell was investigated that exhibited 80 mAh g^{-1} [29].
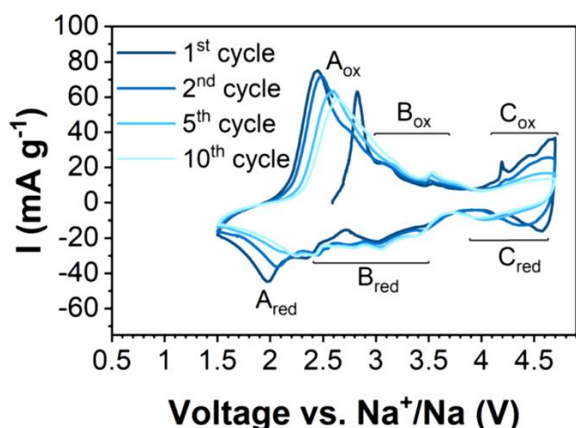

Figure 8. CV curves of $Na_{2.4}Mn_{2.6}Al_{0.4}O_7$ at a scan rate of 0.1 mV s^{-1} in the voltage range 1.5–4.7 V vs. Na+/Na. Reprinted with permission from [30]. Copyright {2021} Royal Society of Chemistry
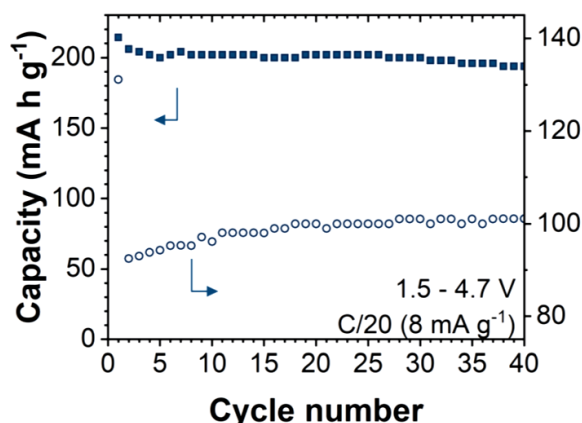

Figure 9. Cycle performance of Al-doped NaMnO in the voltage range 1.5–4.7 V. Reprinted with permission from [30]. Copyright {2021} Royal Society of Chemistry

Soares et al. have studied the effects of partial substitution of Al^{3+} ions in the $Na_2Mn_3O_7$ cathode material. During experiments (Fig. 8), two redox couple of Mn^{3+}/Mn^{4+} and O^2/O^{n-} was confirmed on CV, XANES, and computational studies. The electrochemical characteristics showed the 215 mAh g^{-1} initial capacity between the voltage range 1.5–4.7 at C/20 and 90 % capacity retention after 40 cycles, as shown in Figure 9. Modeled structure gave observation that Al^{3+} is more electronegative than Mn^{4+} which can let diffusion of Na^+ in various directions. And diffusion kinetics can be improved through the shorter length Al-O bond that helps widener the Na^+ pathway [30].

Redox-inactive Ti^{4+} chemistry was investigated by Liu et al. and used to partially substitute Mn^{4+} to form $Na_2Ti_{0.5}Mn_{2.5}O_7$. The results indicate that Ti^{4+} can reduce objectionable interlayer gliding at a high voltage, and this material showed ultra-slow volume change (0.11 %), revealing structure stability. $Na_2Ti_{0.5}Mn_{2.5}O_7$ delivered good cycling performance with 79.1 % capacity retention after 60 cycles at

50 mA·g^{-1}. Moreover, after storing in the air for 60 days, the cyclic stability of $Na_2Ti_{0.5}Mn_{2.5}O_7$ showed 77.0 % capacity retention after 60 cycles which indicates the air stability of doped material [31].

Conclusions

In summary, $Na_2Mn_3O_7$ material is very attractive as a cathode material not only for SIBs due to the low price and high capacity. The manganese redox can be used if the cutoff voltage is limited up to 3V and the capacity of about 160 mAh g^{-1} is delivered. However, due to the Jahn-Telle distortion associated with Mn^{3+}, the cycling performance still needs to be improved. When the cut-off voltage increased over 3 V (up to 4.7 V), the participation of the oxygen redox increased the capacity to over 200 mAh g^{-1}. The enhancement of the cycling performance was done by partial substitution of the manganese with other metals such as Mg, Al, and Ti. Furthermore, coating the material with carbon or other materials is one of the ways to improve cycling performance.

Acknowledgment

References

1   Dunn, B., Kamath, H., & Tarascon, J. M. (2011). Electrical energy storage for the grid: A battery of choices. *Science,* 334, 6058. https://doi.org/10.1126/science.1212741

2   Delmas, C. (2018). Sodium and Sodium-Ion Batteries: 50 Years of Research. *Advanced Energy Materials,* 8, 1703137. https://doi.org/10.1002/aenm.201703137

3   Pan, H., Hu, Y. S., & Chen, L. (2013). Room-temperature stationary sodium-ion batteries for large-scale electric energy storage. *Energy and Environmental Science,* 6, 2338-2360. https://doi.org/10.1039/c3ee40847g

4   Guney, M. S., & Tepe, Y. (2017). Classification and assessment of energy storage systems. *Renewable and Sustainable Energy Reviews,* 75, 1187-1197. https://doi.org/10.1016/j.rser.2016.11.102

5   Amiryar, M. E., & Pullen, K. R. (2017). A review of flywheel energy storage system technologies and their applications. *Applied Sciences,* 7, 3. https://doi.org/10.3390/app7030286

6   Kiehne, H. A. (2003). Battery Technology Handbook. *Battery Technology Handbook.* https://doi.org/10.1201/9780203911853

7   Dehghani-Sanij, A. R., Tharumalingam, E., Dusseault, M. B., & Fraser, R. (2019). Study of energy storage systems and environmental challenges of batteries. *Renewable and Sustainable Energy Reviews,* 104, 192-208. https://doi.org/10.1016/j.rser.2019.01.023

8   May, G. J., Davidson, A., & Monahov, B. (2018). Lead batteries for utility energy storage: A review. *Journal of Energy Storage*, 15, 145-157. https://doi.org/10.1016/j.est.2017.11.008

9   Fang, Y., Xiao, L., Chen, Z., Ai, X., Cao, Y., & Yang, H. (2018). Recent Advances in Sodium-Ion Battery Materials. In *Electrochemical Energy Reviews*, 1, 294–323. https://doi.org/10.1007/s41918-018-0008-x

10 Wood Mac. Site. Features. Shared. View Models. Metadata. Publisher. (2018, August 6). *U.S. Energy Storage Monitor.* Wood Mackenzie. Retrieved August 16, 2022, from https://www.woodmac.com/industry/power-and-renewables/us-energy-storage-monitor/

11 *Energy storage*. Energy. (n.d.). Retrieved September 5, 2022, from https://energy.ec.europa.eu/topics/research-and-technology/energy-storage_en

12 Monconduit, L. (2021). *Na-Ion Batteries*. Wiley-ISTE. https://doi.org/10.1002/9781119818069

13 Rudola, A., Rennie, A. J. R., Heap, R., Meysami, S. S., Lowbridge, A., Mazzali, F., Sayers, R., Wright, C. J., & Barker, J. (2021). Commercialization of high energy density sodium-ion batteries: Faradion's journey and outlook. *Journal of Materials Chemistry A*, 9, 8279-8302. https://doi.org/10.1039/d1ta00376c

14 Deng, J., Luo, W. bin, Chou, S. L., Liu, H. K., & Dou, S. X. (2018). Sodium-Ion Batteries: From Academic Research to Practical Commercialization. *Advanced Energy Materials,* 8, 1701428. https://doi.org/10.1002/aenm.201701428

15 Adamczyk, E., & Pralong, V. (2017). $Na_2Mn_3O_7$: A Suitable Electrode Material for Na-Ion Batteries? *Chemistry of Materials*, *29*(11), 4645–4648.

16 Raekelboom, E. A., Hector, A. L., Owen, J., Vitins, G., & Weller, M. T. (2001). Syntheses, structures, and preliminary electrochemistry of the layered lithium and sodium manganese (IV) oxides, $A_2Mn_3O_7$. *Chemistry of Materials*, *13*(12), 4618–4623. https://doi.org/10.1002/chin.200208006

17 Sada, K., & Barpanda Prabeer, B. (2019). Layered Sodium Manganese Oxide $Na_2Mn_3O_7$ as an Insertion Host for Aqueous Zinc-ion Batteries. *MRS Advances*, *4*(49), 2651-2657. https://doi.org/10.1557/adv.2019.297

18 Sada, K., Senthilkumar, Baskar Ritambhara Gond, S., Pralong, V., & Barpanda, P. B. (2021). Layered $Na_2Mn_3O_7$: A Robust Cathode for Na, K, and Li-Ion Batteries. *Recent Research Trends in Energy Storage Devices*. https://doi.org/10.1007/978-981-15-6394-2

19 Sada, K., Senthilkumar, B., & Barpanda, P. (2018). Layered $Na_2Mn_3O_7$ as a 3.1 V Insertion Material for Li-Ion Batteries. *ACS Applied Energy Materials*, *1*(12), 6719–6724.

20 Yabuuchi, N., Takeuchi, M., Nakayama, M., Shiiba, H., Ogawa, M., Nakayama, K., Ohta, T., Endo, D., Ozaki, T., Inamasu, T., Sato, K., & Komaba, S. (2015). High-capacity electrode materials for rechargeable lithium batteries: Li_3NbO_4-based system with cation-disordered rocksalt structure. *Proceedings of the National Academy of Sciences of the United States of America*, *112*(25). https://doi.org/10.1073/pnas.1504901112

21 Koga, H., Croguennec, L., Ménétrier, M., Douhil, K., Belin, S., Bourgeois, L., Suard, E., Weill, F., & Delmas, C. (2013). Reversible Oxygen Participation to the Redox Processes Revealed for $Li_{1.20}Mn_{0.54}Co_{0.13}Ni_{0.13}O_2$. *Journal of The Electrochemical Society*, *160*(6). https://doi.org/10.1149/2.038306jes

22 Seo, D. H., Lee, J., Urban, A., Malik, R., Kang, S., & Ceder, G. (2016). The structural and chemical origin of the oxygen redox activity in layered and cation-disordered Li-excess cathode materials. *Nature Chemistry*, *8*(7). https://doi.org/10.1038/nchem.2524

23 Mortemard De Boisse, B., Liu, G., Ma, J., Nishimura, S. I., Chung, S. C., Kiuchi, H., Harada, Y., Kikkawa, J., Kobayashi, Y., Okubo, M., & Yamada, A. (2016). Intermediate honeycomb ordering to trigger oxygen redox chemistry in layered battery electrode. *Nature Communications*, *7*. https://doi.org/10.1038/ncomms11397

24 Yabuuchi, N., Nakayama, M., Takeuchi, M., Komaba, S., Hashimoto, Y., Mukai, T., Shiiba, H., Sato, K., Kobayashi, Y., Nakao, A., Yonemura, M., Yamanaka, K., Mitsuhara, K., & Ohta, T. (2016). Origin of stabilization and destabilization in solid-state redox reaction of oxide ions for lithium-ion batteries. *Nature Communications*, *7*. https://doi.org/10.1038/ncomms13814

25 Mortemard de Boisse, B., Nishimura, S., Watanabe, E., Lander, L., Tsuchimoto, A., Kikkawa, J., & Yamada, A. (2018). Highly Reversible Oxygen-Redox Chemistry at 4.1 V in Na4/7− x [□1/7 Mn6/7]O2 (□: Mn Vacancy). *Advanced Energy Materials*, 8(20), 1800409. http://doi:10.1002/aenm.201800409

26 Tsuchimoto, A., Shi, X. M., Kawai, K., Mortemard de Boisse, B., Kikkawa, J., Asakura, D., Okubo, M., & Yamada, A. (2021). Nonpolarizing oxygen-redox capacity without O-O dimerization in $Na_2Mn_3O_7$. *Nature Communications*, *12*(1). https://doi.org/10.1038/s41467-020-20643-w

27 House, R. A., Maitra, U., Pérez-Osorio, M. A., Lozano, J. G., Jin, L., Somerville, J. W., Duda, L. C., Nag, A., Walters, A., Zhou, K. J., Roberts, M. R., & Bruce, P. G. (2020). Superstructure control of first-cycle voltage hysteresis in oxygen-redox cathodes. *Nature*, *577*(7791). https://doi.org/10.1038/s41586-019-1854-3

28 Tran, N., Croguennec, L., Ménétrier, M., Weill, F., Biensan, P., Jordy, C., & Delmas, C. (2008). Mechanisms associated with the "plateau" observed at high voltage for the overlithiated $Li_{1.12}(Ni_{0.425}Mn_{0.425}Co_{0.15})_{0.88}O_2$ system. *Chemistry of Materials*, *20*(15). https://doi.org/10.1021/cm070435m

29 Siriwardena, D. P., Fernando, J. F. S., Wang, T., Firestein, K. L., Zhang, C., Brand, H. E. A., Jones, M. W. M., Kewish, C. M., Berntsen, P., Jenkins, T., Lewis, C. E. M., von Treifeldt, J. E., Dubal, D. P., & Golberg, D. v. (2021). Probing the effect of Mg doping on triclinic $Na_2Mn_3O_7$ transition metal oxide as cathode material for sodium-ion batteries. *Electrochimica Acta*, *394*. https://doi.org/10.1016/j.electacta.2021.139139

30 Soares, C., Silván, B., Choi, Y. S., Celorrio, V., Seymour, V. R., Cibin, G., Griffin, J. M., Scanlon, D. O., & Tapia-Ruiz, N. (2021). $Na_{2.4}Al_{0.4}Mn_{2.6}O_7$ anionic redox cathode material for sodium-ion batteries — a combined experimental and theoretical approach to elucidate its charge storage mechanism. *Journal of Materials Chemistry A*, *10*(13). https://doi.org/10.1039/d1ta05137g

31 Liu, Y., Wang, C., Ren, M., Fang, H., Jiang, Z., & Li, F. (2021). Ultralow-strain Ti substituted Mn-vacancy layered oxides with enhanced stability for sodium-ion batteries. *Journal of Energy Chemistry*, *63*. https://doi.org/10.1016/j.jechem.2021.07.024

Information about authors*

Rakhymbay, Lunara — PhD student, School of Engineering and Digital Sciences, Nazarbayev University, Kabanbay Batyr Ave., 53, Astana, Kazakhstan; *e-mail:* lunara.rakhymbay@nu.edu.kz; https://orcid.org/0000-0002-7924-837X;

Shugay, Bagdaulet — Research Assistant, School of Engineering and Digital Sciences, Nazarbayev University, Kabanbay Batyr Ave., 53, Astana, Kazakhstan; e-mail: bagdaulet.shugay@alumni.nu.edu.kz; https://orcid.org/0000-0002-3564-432X;

Karlykan, Maksat — Undergraduate student, Department of Chemical and Materials Engineering, School of Engineering and Digital Sciences, Nazarbayev University, Kabanbay Batyr Ave., 53, Astana, Kazakhstan; e-mail: maksat.karlykan@nu.edu.kz;

Namazbay, Alibi — Undergraduate student, Department of Chemical and Materials Engineering, School of Engineering and Digital Sciences, Nazarbayev University, Kabanbay Batyr Ave., 53, Astana, Kazakhstan; e-mail: alibi.namazbay@nu.edu.kz;

Konarov, Aishuak (*corresponding author*) — Assistant Professor, Department of Chemical and Materials Engineering, School of Engineering and Digital Sciences, Nazarbayev University, Kabanbay Batyr Ave., 53, Astana, Kazakhstan; e-mail: aishuak.konarov@nu.edu.kz; https://orcid.org/0000-0001-9352-8602;

Bakenov, Zhumabay — Professor, Department of Chemical and Materials Engineering, School of Engineering and Digital Sciences, Nazarbayev University, Kabanbay Batyr Ave., 53, Astana, Kazakhstan; e-mail: zbakenov@nu.edu.kz; https://orcid.org/0000-0003-2781-4955

_____

*The author's name is presented in the order: *Last Name, First and Middle Names*